Electronic Supplementary Information

Synthesis, structure, solution behavior, reactivity and biological evaluation of oxidovanadium(IV/V) thiosemicarbazone complexes.

Saswati,[a] Pedro Adão,[b] Sudarshana Majumder,[a,c] Subhashree P. Dash,[a,d] Satabdi Roy,[a,e] Maxim L. Kuznetsov,[b] João Costa Pessoa,[b,*] Clara S. B. Gomes,[b] Manasi R. Hardikar,[f] Edward R. T. Tiekink[g] and Rupam Dinda*[a]

[a]*Department of Chemistry, National Institute of Technology, Rourkela 769008, Odisha, India*

[b]Centro de Química Estrutural, Instituto Superior Técnico, Universidade de Lisboa, Av. Rovisco Pais, 1049-001 Lisboa, Portugal

[c]*Darmstadt University of Technology, Clemens-Schöpf Institute of Organic Chemistry and Biochemistry, Alarich-Weiss Str. 4, 64287 Darmstadt, Germany.*

[d]*Department of Basic Sciences, Parala Maharaja Engineering College, Sitalapalli, Brahmapur, Odisha 761003, India*

[e]*Department of Chemistry, Indian Institute of Technology, Kanpur 208016, Uttar Pradesh, India.*

[f]*Biometry and Nutrition Group, Agharkar Research Institute, G.G. Agrakar Road, Pune 411004*

[g]*Research Centre for Crystalline Materials, School of Science and Technology, Sunway University, Bandar Sunway, Selangor Darul Ehsan 47500, Malaysia*

Table of Contents

Table S1. Selected bond distances (Å) and angles (°) for compound 3.

	3	
	molecule A	molecule B
Distances (Å)		
S1–C2	1.710(6)	1.714(7)
C2–N2	1.307(9)	1.297(9)
N2–N1	1.355(8)	1.374(8)
N1–C1	1.339(9)	1.305(8)
C1–S1	1.735(8)	1.738(8)
C1–N4	1.332(9)	1.348(9)
N4–C8	1.420(9)	1.370(8)
C2–C3	1.465(10)	1.443(10)
Angles (º)		
C2–S1–C1	87.4(4)	87.1(3)
C2–N2–N1	113.5(5)	114.3(5)
N2–N1–C1	112.1(6)	111.1(6)
N1–C1–S1	112.7(6)	114.0(5)
C1–N4–C8	131.8(7)	132.6(7)
N2–C2–S1	114.2(5	113.4(5)

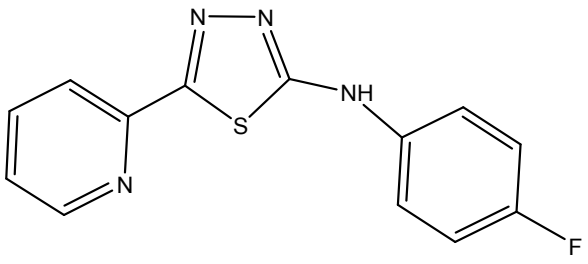

Fig. S1. Representation of compound **3**.

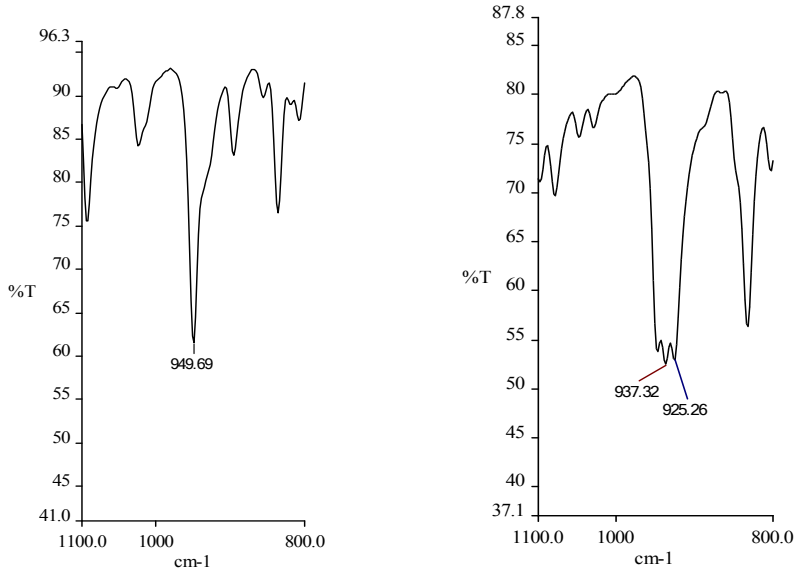

(a) (b)

Fig. S2. FTIR spectra of (a) [$V^{IV}O(L)(acac)$] (**1**) and (b) [$V^{V}O_2(L')$] (**2**) showing the (V=O) stretching bands.

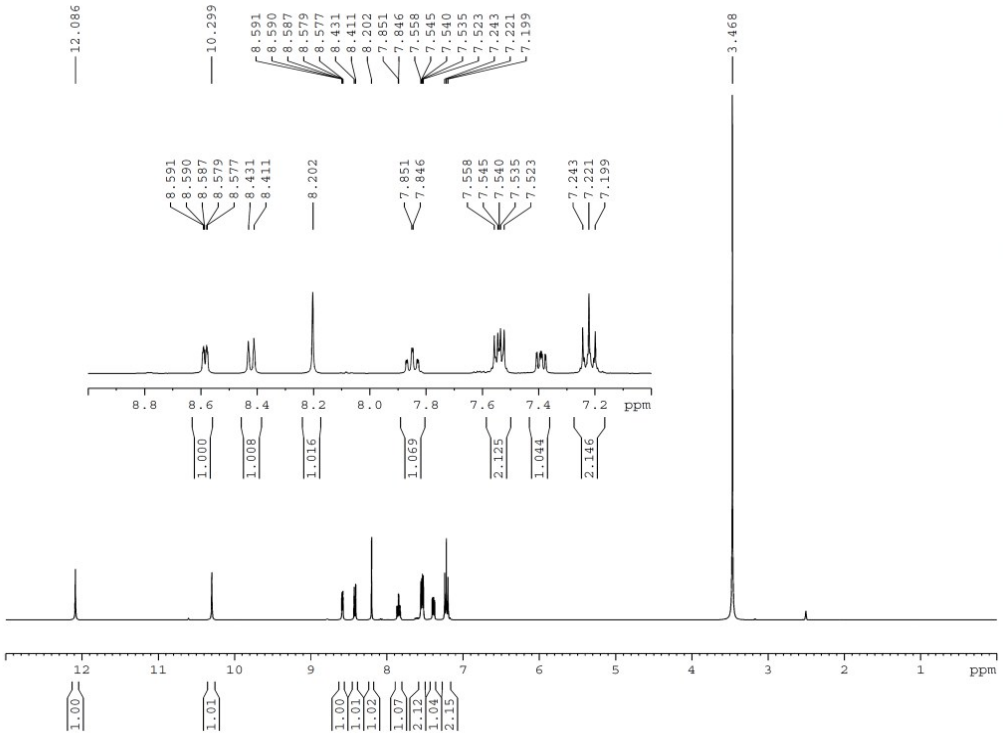

Fig. S3. ^{1}H NMR spectra of ligand HL (60 mM) in DMSO–d_6.

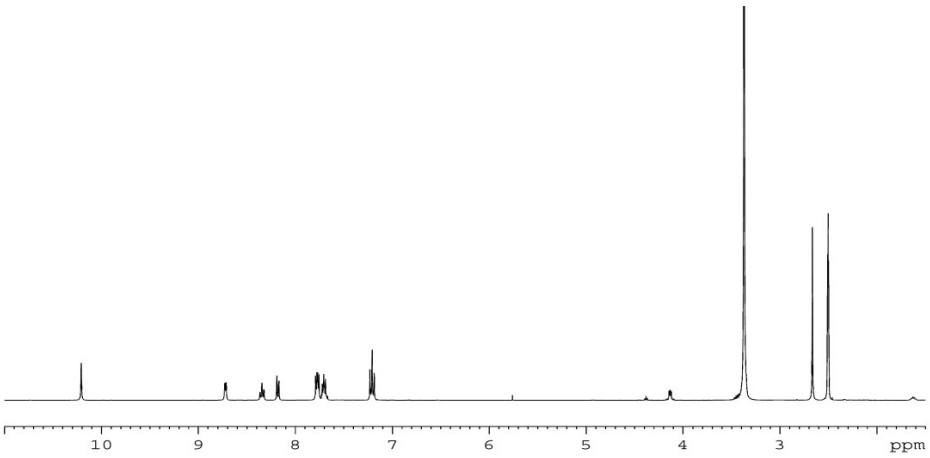

Fig. S4. ^{1}H NMR spectrum of complex [$V^{V}O_2$(L´)] (**2**) (60 mM) in DMSO–d_6.

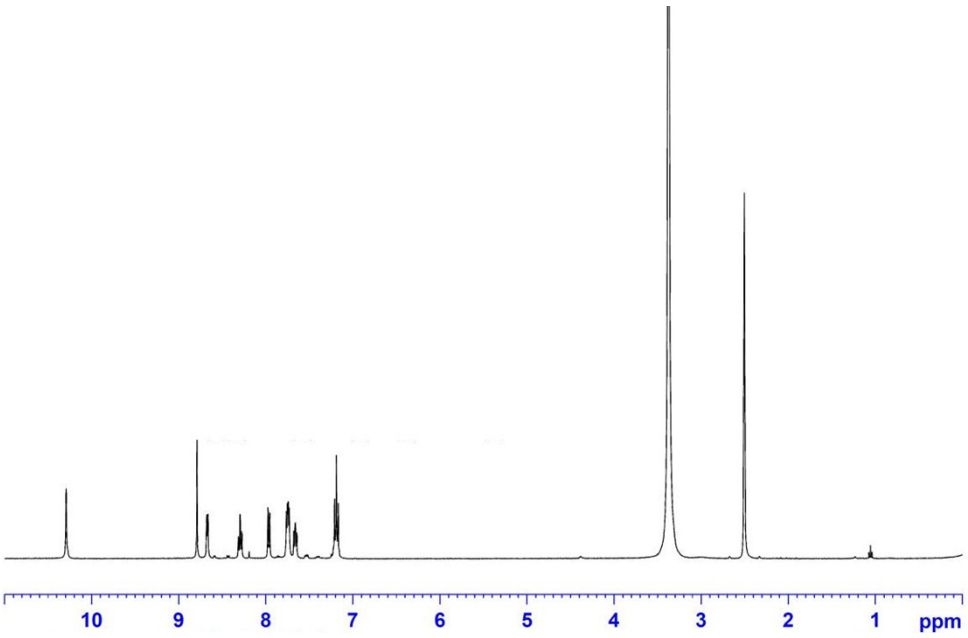

Fig. S5. ^{1}H NMR spectra of [$V^{V}O_2$(L)] (**2a**) in DMSO–d_6.

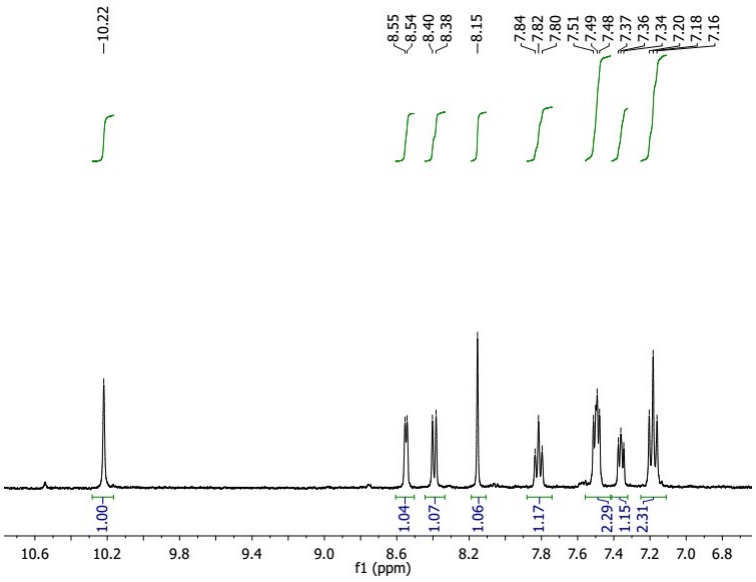

Fig. S6, ^{1}H NMR spectrum of HL (ca. 32 mM) in DMSO after 24 h at 60^{o}C.

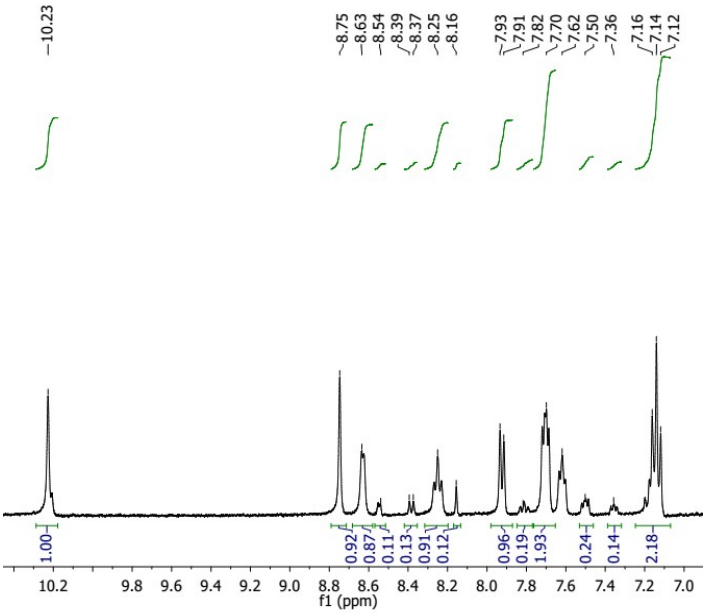

Fig. S7 ^{1}H NMR spectrum of HL with $V^{V}O(OiPr)_3$ in DMSO after 1 h at room temperature, with an additional 30 min at 60°C. Reagent concentration was ca. 90 mM.

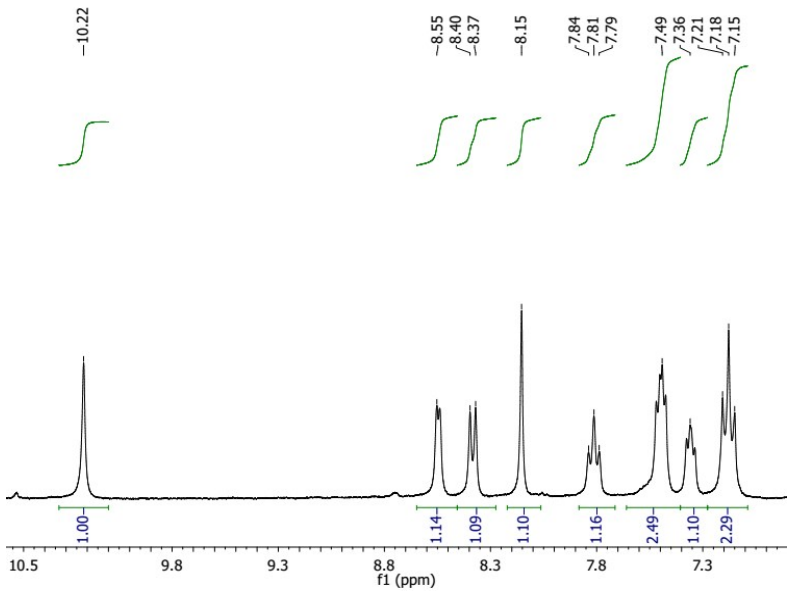

Fig. S8. ^{1}H NMR spectrum of HL with $V^{IV}OSO_4$ in DMSO, after 20 min at 60°C. Reagent concentrations were ca. 9 mM.

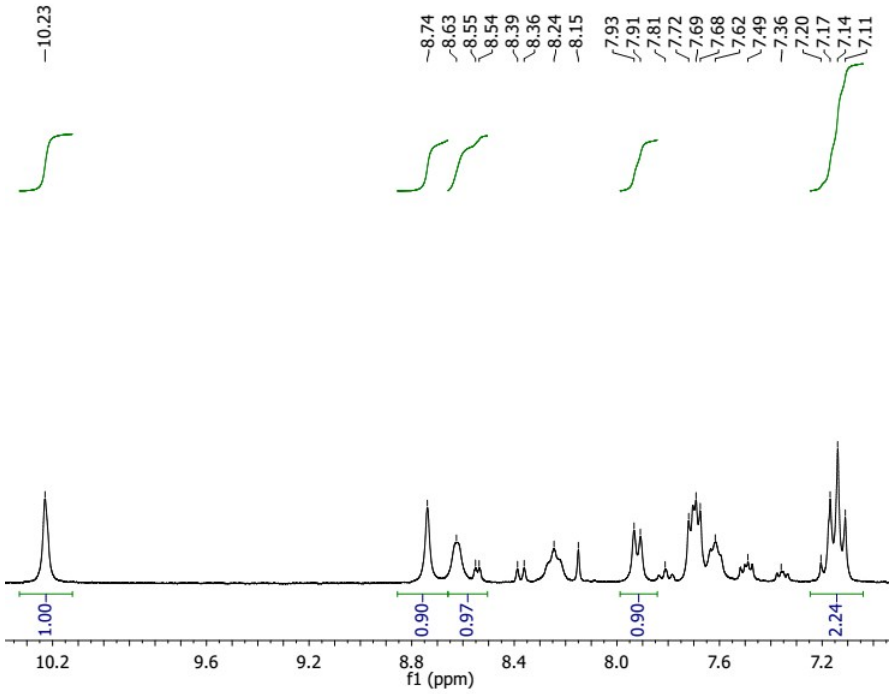

Fig. S9. ^{1}H NMR spectrum of HL with $V^{V}O(OiPr)_3$ in DMSO after 1 h at room temperature with an additional 3 h at 60°C. Reagent concentration was ca. 90 mM.

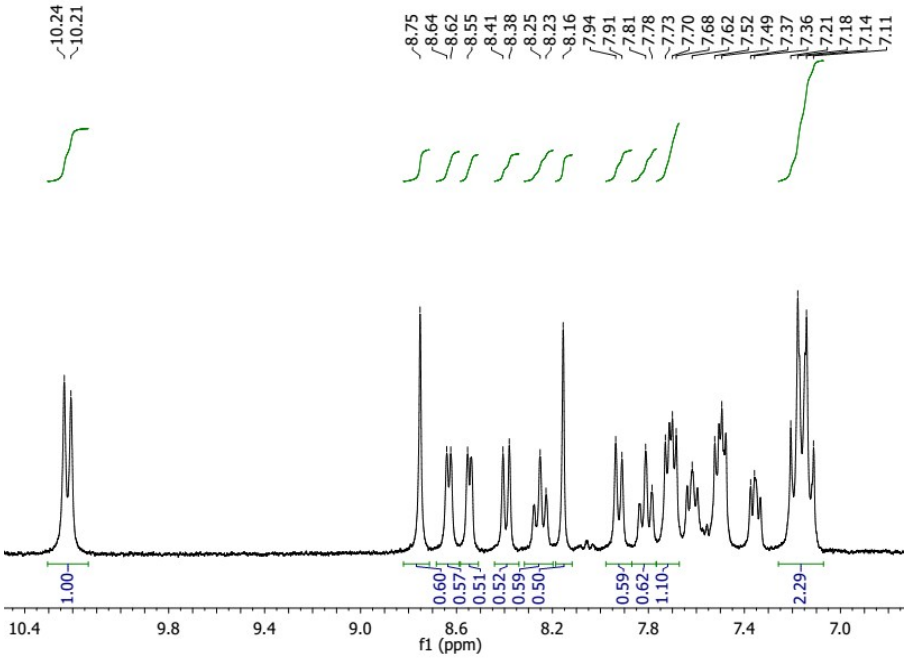

Fig. S10. ^{1}H NMR spectrum of HL with $V^{V}O(OiPr)_3$ and acetylacetone (1:1:1) in DMSO after dissolution of the reagents at room temperature. Reagent concentrations were ca. 0.18 M.

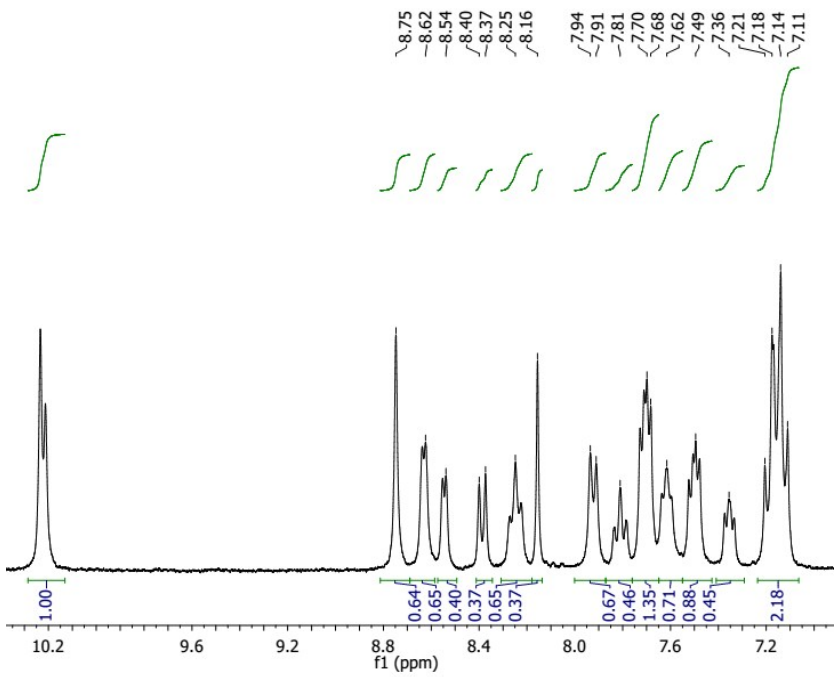

Fig. S11. ^{1}H NMR spectrum of HL with $V^{V}O(OiPr)_3$ and acetylacetone (1:1:1) in DMSO after 20 min at 60^{o}C. Reagent concentrations were ca. 0.18 M.

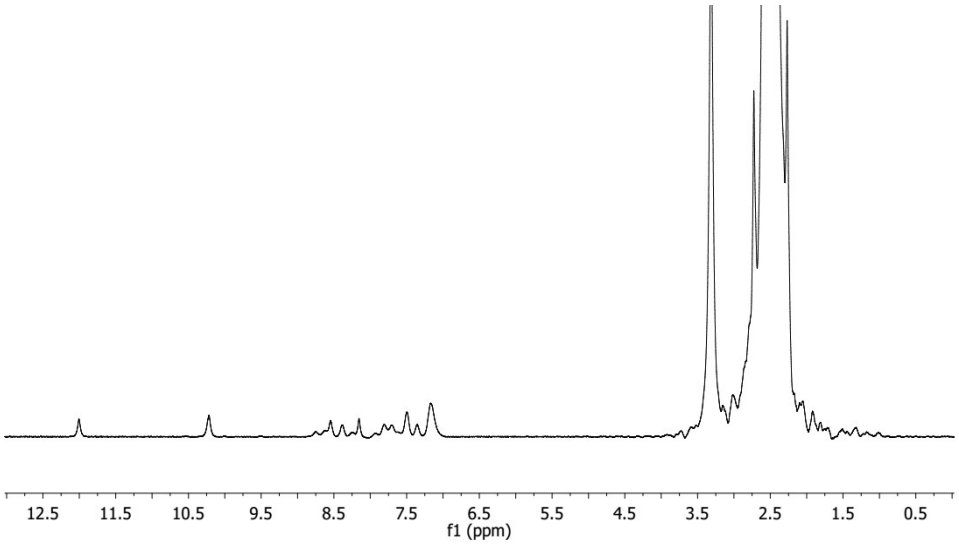

Fig. S12. ^{1}H NMR spectrum of **1** (ca. 0.19 M) in DMSO, after heating for 10 min at 60^{o}C and cooling down for 2 h to room temperature.

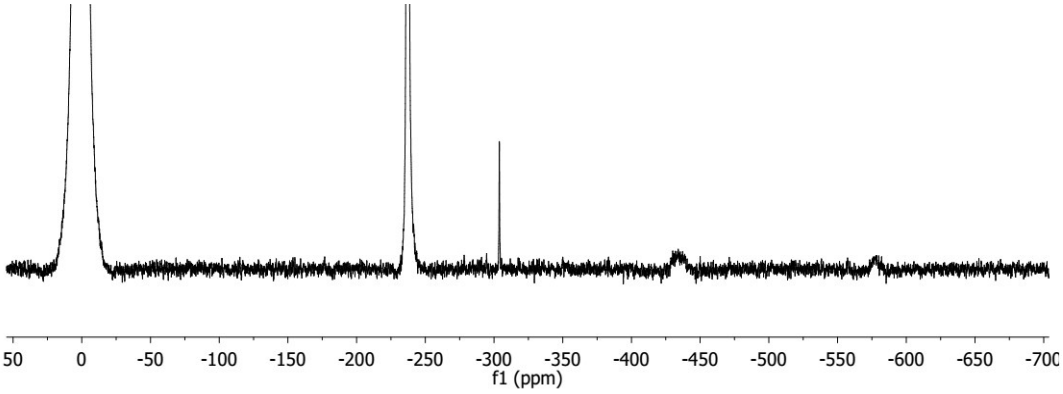

Fig. S13. ^{51}V NMR spectrum of **1** in DMSO after heating for 10 min at 60^{o}C and cooling down for 2 h to room temperature. Concentration of **1** was ca. 0.19 M.

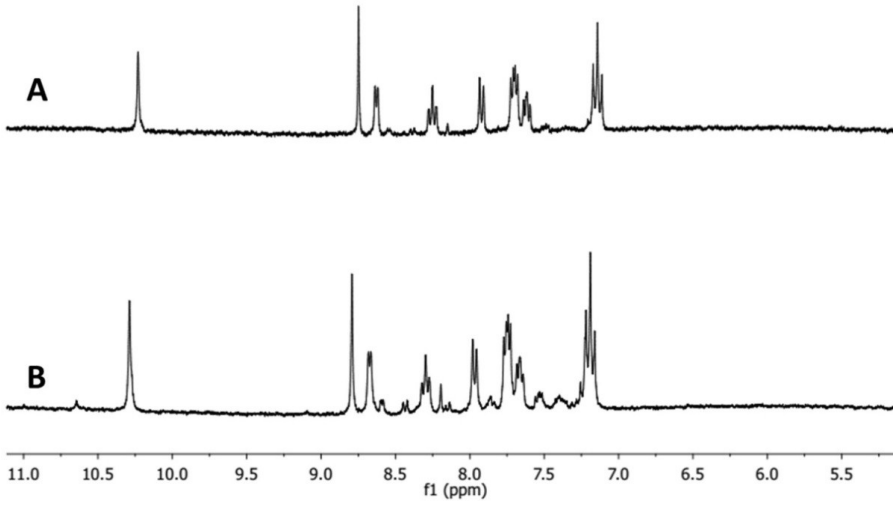

Fig. S14 ^{1}H NMR spectra of **2a** (ca. 11 mM) in DMSO after 10 min at 60 ºC (A) and of another spectrum which was measured after 24 h at 60 ^{o}C (B).

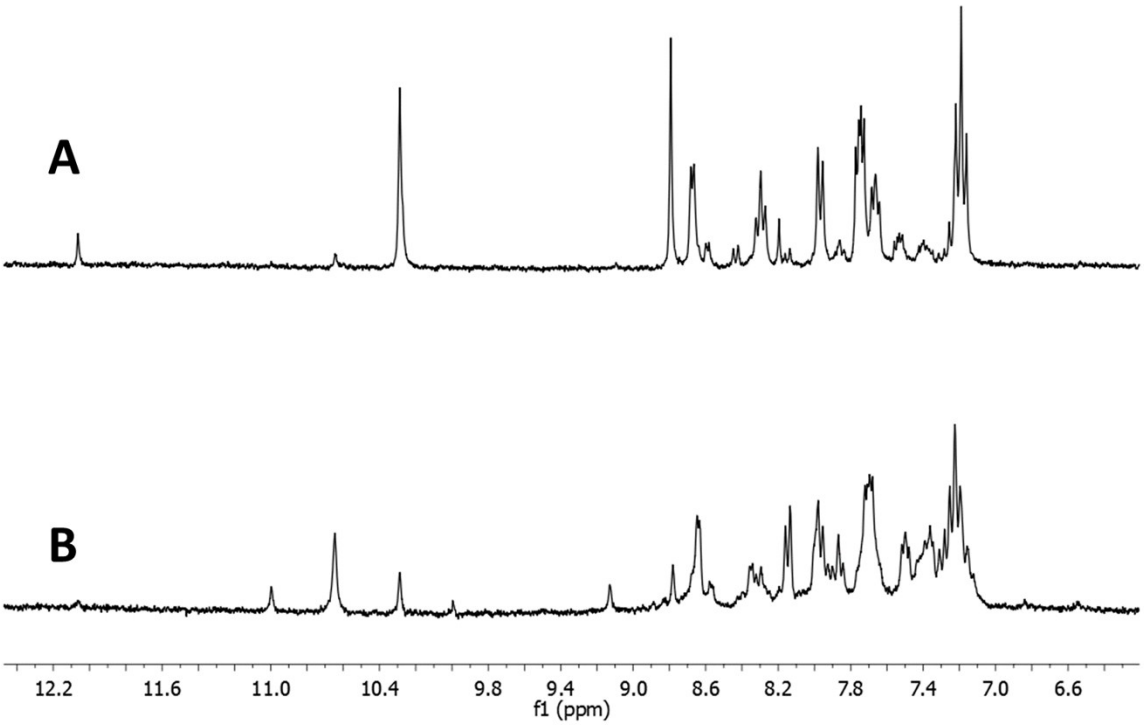

Fig. S15. ^{1}H NMR spectra of complex [$V^{V}O_2$(L)] (**2a**, 25 mM) in DMSO after (A) 24 h and (B) 5 days at 60 ^{o}C.

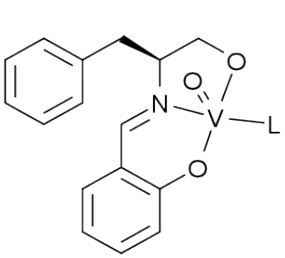

C1

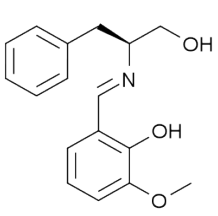

L1

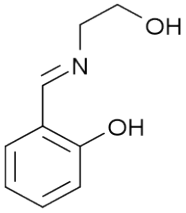

L2

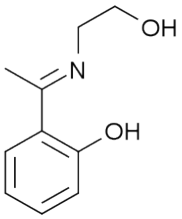

L3

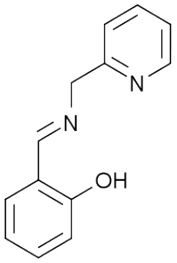

L4

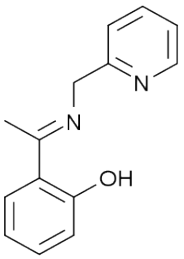

L5

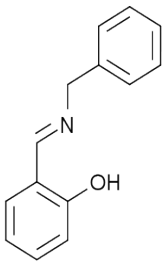

L6

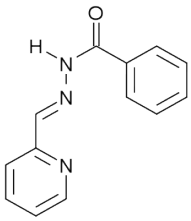

L7

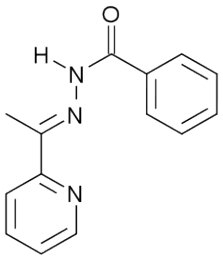

L8

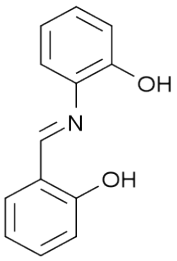

L9

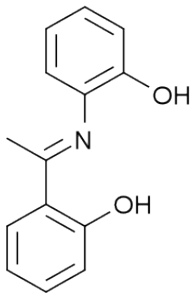

L10

Chart S1. Structural formulas of the ligands and $V^{IV}O$ complex tested in attempts for the alkylation reaction with DMSO. Compound C1 was prepared as reported in the literature. [81e] The L ligand in C1 refers to a coordinated solvent molecule, in this case, DMSO or water.

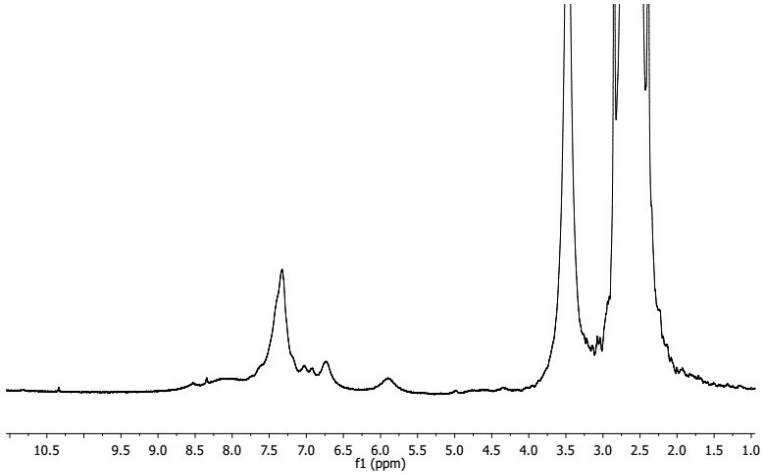

Fig. S16. ^{1}H NMR spectrum of C1 (ca. 50 mM) in DMSO after 1 h at 60^{o}C.

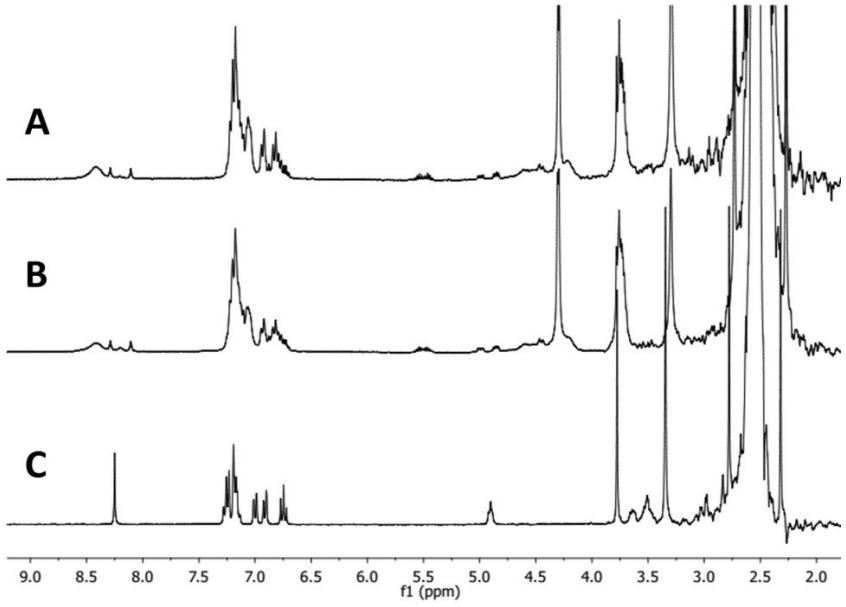

Fig. S17. (A) ^{1}H NMR spectra of a 1:1 mixture of L1 and $V^{V}O(OiPr)_3$ in DMSO after 10 min at 60 ^{o}C; (B) 1:1 mixture of L1 and $V^{V}O(OiPr)_3$ in DMSO at room temperature before heating; (C) L1 in DMSO at room temperature. Reagent concentrations were ca. 0.13 M.

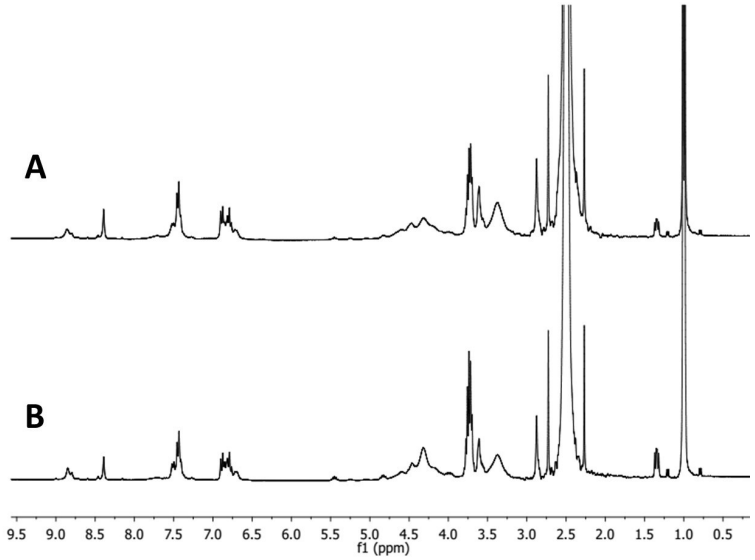

Fig. S18. (A) ^{1}H NMR spectra of a 1:1 mixture of L2 and $V^{V}O(OiPr)_3$ in DMSO after 30 min at 60 ^{o}C; (B) 1:1 mixture of L2 and $V^{V}O(OiPr)_3$ in DMSO at room temperature before heating. Reagent concentration was ca. 0.25 M.

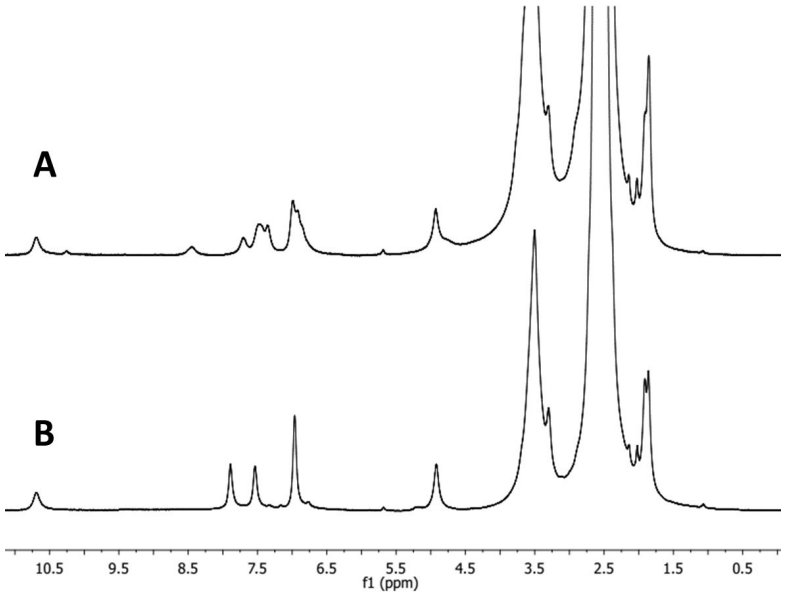

Fig. S19. (A) ^{1}H NMR spectra of a 1:1 mixture of L2 and $V^{IV}O(acac)_2$ in DMSO after 1 h at 60^{o}C; (B) 1:1 mixture of L3 and $V^{IV}O(acac)_2$ in DMSO after 1 h at 60^{o}C. Reagent concentrations were ca. 0.25 M.

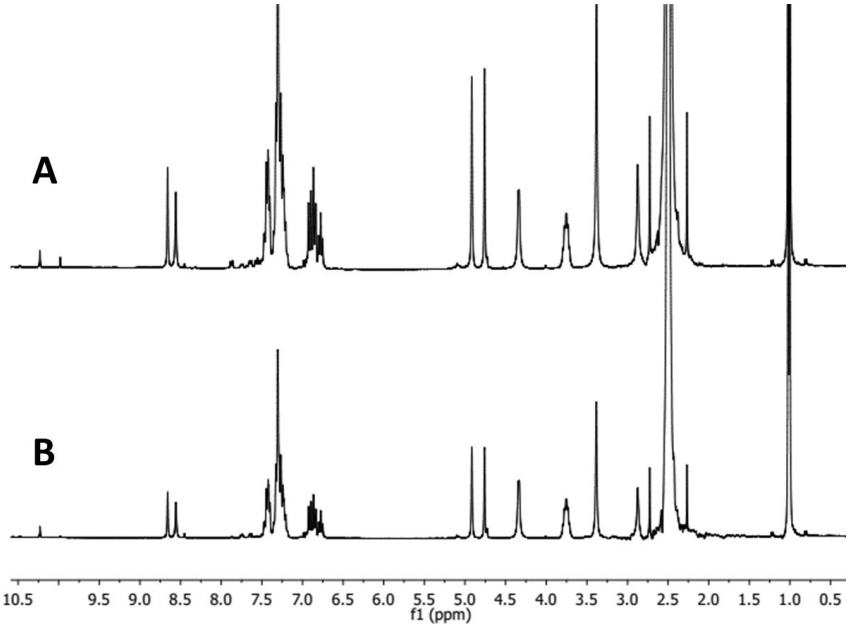

Fig. S20. (A) ^{1}H NMR spectra of a 1:1 mixture of L6 and $V^{V}O(OiPr)_3$ in DMSO after 30 min. at 60^{o}C; (B) 1:1 mixture of L6 and $V^{V}O(OiPr)_3$ in DMSO at room temperature. Reagent concentration were ca. 0.25 M.

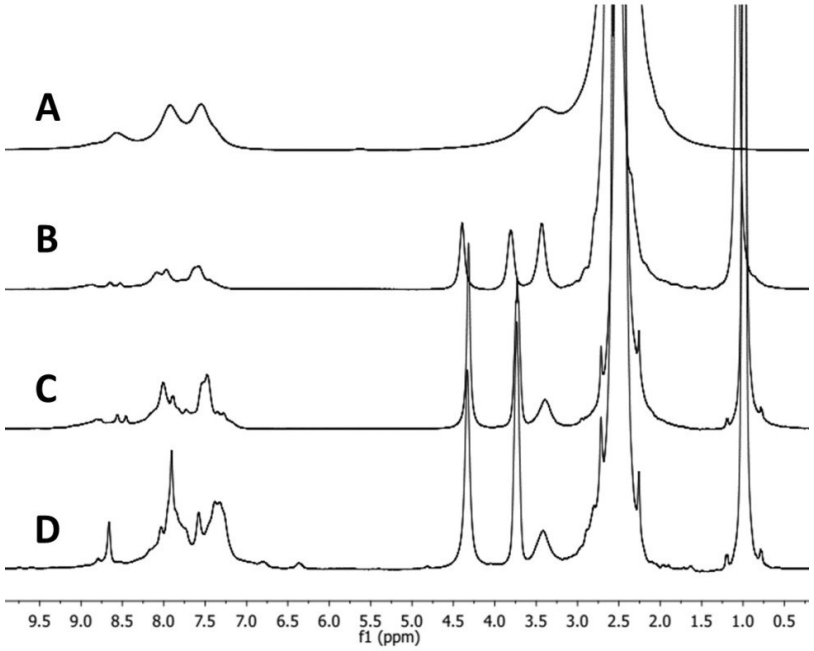

Fig. S21. (A) ^{1}H NMR spectra of a 1:1 mixture of L7 and $V^{IV}O(acac)_2$ in DMSO after 1 h at 60^{o}C; (B) 1:1 mixture of L7 and $V^{V}O(OiPr)_3$ in DMSO after 1 h at 60^{o}C; (C) 1:1 mixture of L7 and $V^{V}O(OiPr)_3$ in DMSO at room temperature; (D) 1:1 mixture of L8 and $V^{V}O(OiPr)_3$ in DMSO at room temperature. Reagent concentrations were ca. 0.25 M.

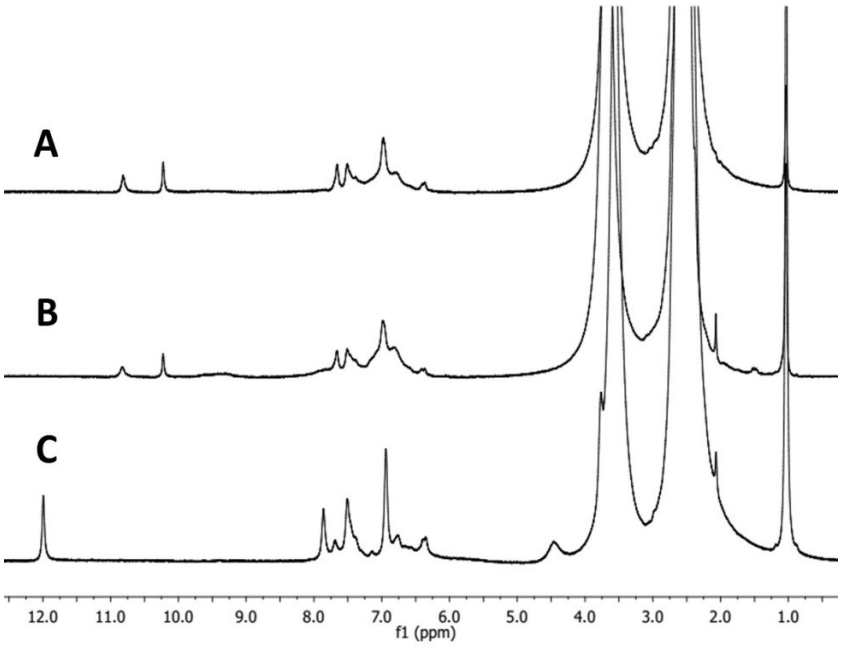

Fig. S22. (A) ^{1}H NMR spectra of a 1:1 mixture of L9 and $V^{V}O(OiPr)_3$ in DMSO after 1 h at 60^{o}C; (B) 1:1 mixture of L7 and $V^{V}O(OiPr)_3$ in DMSO at room temperature; (C) 1:1 mixture of L10 and $V^{V}O(OiPr)_3$ in DMSO at room temperature. Reagent concentrations were ca. 0.5 M.

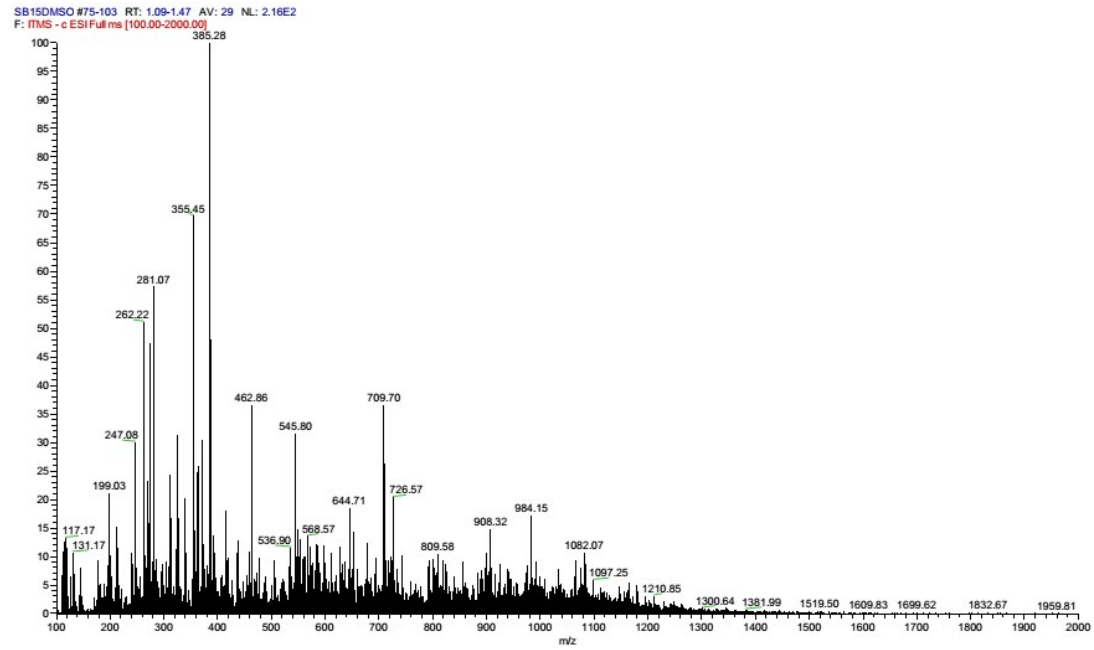

Fig. S23 Negative mode ESI-MS spectrum of **1** in DMSO after 10 min at 60 ºC and ca. 2 h at room temperature. The sample was diluted in methanol.

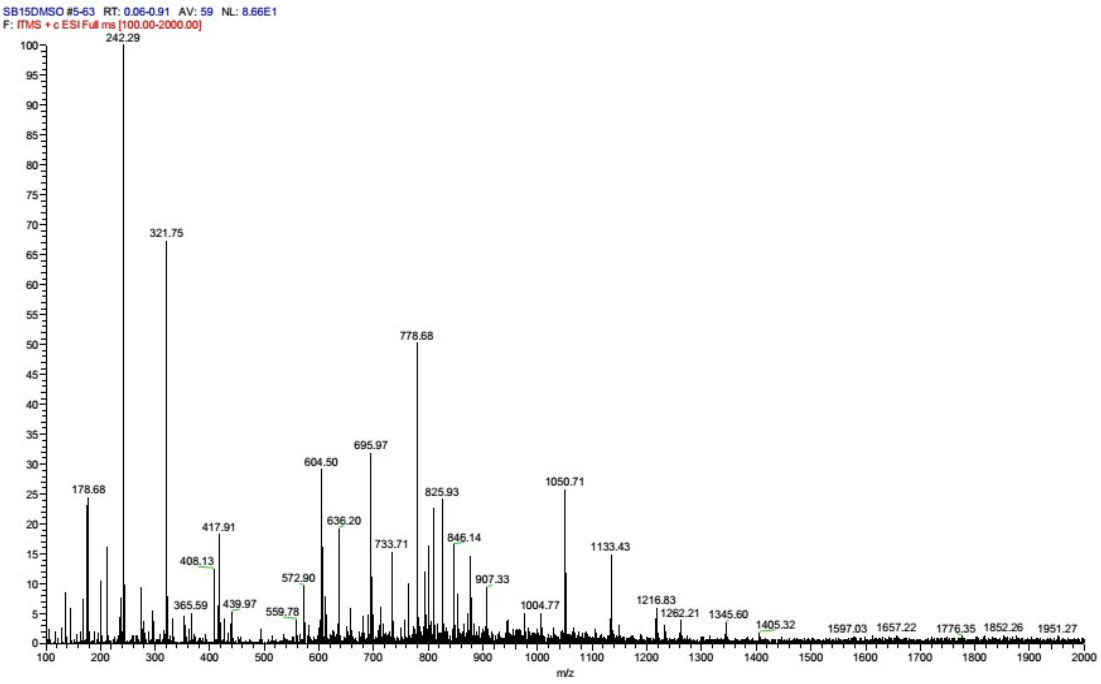

Fig. S24 Positive mode ESI-MS spectrum of **1** in DMSO after 10 min at 60ºC and ca. 2 h at room temperature. The sample was diluted in methanol.

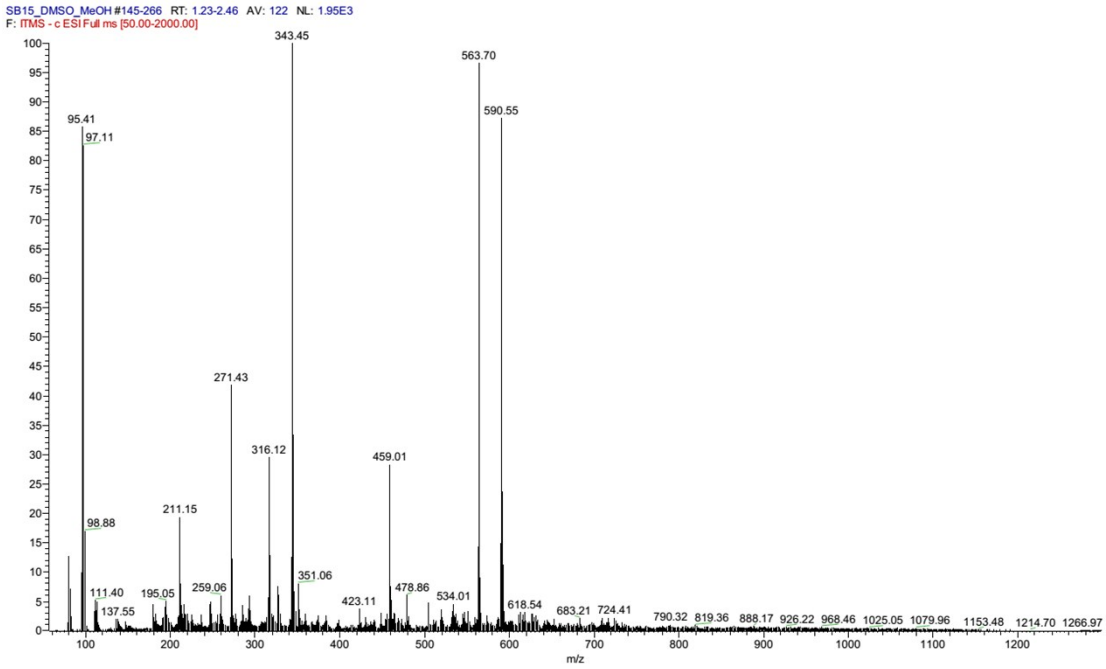

Fig. S25. Negative mode ESI-MS spectrum of **1** after 5 days in DMSO at 60 ^{o}C.

The observation of methanesulfenic acid or methanesulfenate anion is difficult under the conditions used, given its high reactivity. Instead, we sought to observe methanesulfonic acid (MW= 96), as it is the most likely decomposition product of the sulfenic acid. It should be noted that m/z = 96 is below the normal detection limit of the equipment (m/z=100), but nevertheless, in the rare ESI-MS spectra recorded with data below m/z of 100, we detected a peak (negative mode at m/z = 95, ca. 85%, Fig. S25), which could be tentatively attributed to $CH_3SO_3^-$.

Most of our ESI spectra are for m/z > 100, so we also attempted to search for possible adducts with DMSO and/or MeOH in both positive and negative ESI-MS spectra. The only peaks to which some assignment can possibly be made is at ESI(-)-MS m/z=131 (($MeSO_3^-.2H_2O$), ca.10%, Fig S23) and ESI(+)-MS m/z=178.8, corresponding to $[H(MeSO_3H.2MeOH.H_2O)]^+$ (ca. 25%, Fig. S24) in the positive mode. Given the low abundance and low mass of these peaks, along with the high noise of the ESI(-) spectrum, we refrained from making assignments to these signals in the main text.

Two independent molecules comprise the asymmetric unit of **3**, S26 (a), and these adopt very similar conformations as seen in the overlay diagram in Fig. S26 (b). The five-membered ring is strictly planar (r.m.s. deviation = 0.002 Å) and this forms dihedral angles of 13.1(4) and 1.5(3)° with the 4-fluorophenylamine and pyridyl substituents, respectively, reflecting a small twist about the N1–C8 bond as seen in the value of the C1–N1–C8–C9 torsion angle of 11.4(16)°; the dihedral angle between the outer substituents is 12.6(5)°. The second independent molecule is considerably more planar with the dihedral angles between the 1,3,4-thiadiazolyl ring and 4-fluorophenylamine and 2-pyridyl groups being 2.5(5) and 0.8(4)°. In each molecule, the pyridyl-N4 atom is orientated to be proximate to the ring-S1 atom with the S1···N4 separation of 2.945(8) Å (2.953(8) Å for the second molecule) suggestive of attractive contacts[Ref S1] consistent with the observed planar relationship between the 1,3,4-thiadiazolyl and pyridyl rings.

(Ref S1. B. R. Beno, K.-S. Yeung, M. D. Bartberger, L. D. Pennington and N. A. Meanwell, *J. Med. Chem.,* 2015*,* **58**, 4383.)

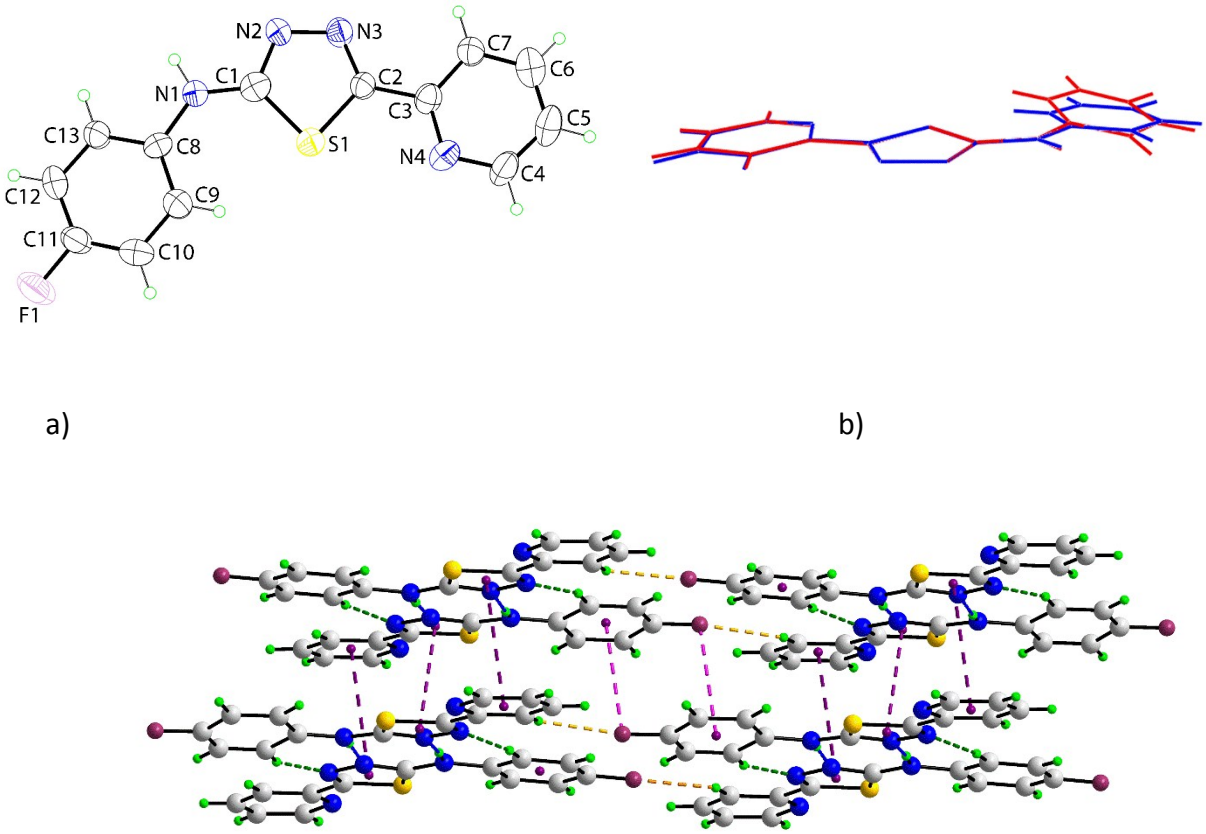

Fig. S26. Crystallographic diagrams for **3**: (a) Molecular structure of the second independent molecule (molecule A) comprising the asymmetric unit of **3**, show atom labelling and displacement ellipsoids at the 35% probability level. (b) Overlay diagram of the first (red image) and the second (blue) independent molecules comprising the asymmetric unit of **3**. The molecules have been overlapped so that the five-membered rings are coincident. (c) Supramolecular double-chain in the molecular packing. Details of the supramolecular association: N–H…N interactions (blue dashed lines) N1a–H1an···N2 = 2.03(6) Å, N1a···N2 = 2.904(10) Å and angle at H1an = 173(6)°; N1–H1n···N2a = 2.04(7) Å, N1···N2a = 2.916(10) Å and angle at H1n = 174(8)°. C–H···N interactions (green dashed lines) C13a–H13a···N3 = 2.60 Å, C13a···N3 = 3.514(11) Å and angle at H13a = 169°. C–H···F interactions (orange dashed lines) C7–H7···F1^{i} = 2.55 Å, C7···F1^{i} = 3.263(11) Å and angle at 134°; C7a–H7a···F1a^{ii} = 2.54 Å, C7a···F1a^{ii} = 3.287(10) Å and angle at H7a = 137°. C–F···π interactions (pink dashed lines) C11–F1···Cg(C8-C13)^{iii} = 3.449(8) Å, C11···Cg(C8-C13)^{iii} = 3.827(10) Å and angle at F1 = 95.3(5)°. C–H···π interactions (brown dashed lines) C4a–H4a···Cg(C8-C13)^{iv} = 2.83 Å, C4a···Cg(C8-C13)^{iv} = 3.575(10) Å and angle at H4a = 138°; C5–H5···Cg(C8a-C13a)^{v} = 2.96 Å, C5···Cg(C8a-C13a)^{v} = 3.683(12) Å and angle at H5 = 136°. π···π interactions (purple

dashed lines) Cg(S1,N2,N3,C1,C2)···Cg(S1,N2,N3,C1,C2)^{vi} = 3.453(4) Å and angle of inclination = 0°; Cg(N4,C3-C7)···Cg(S1a,N2a,N3a,C1a,C2a)^{vi} = 3.661(5) Å and angle of inclination = 3.0(4)°. Symmetry operations - *i*: *x*, *y*, -1+*z*; *ii*: *x*, *y*, 1+*z*; *iii*: 2-*x*, -*y*, 2-*z*; *iv*: 1-*x*, ½+*y*, 1½-*z*; *v*: 2-*x*, -½+*y*, ½-*z*; *vi*: 2-*x*, -*y*, 1-*z*.

Molecular packing

In the crystal of **2** supramolecular chains aligned along the *a*-axis and with a zigzag topology are formed through amine-N–H···O(oxido) hydrogen bonding, Fig. S27 (a); details of the intermolecular interactions are given in the caption to Fig. S28. Chains are consolidated into the three dimensional architecture by a combination of pyridyl-C–H···O(oxido) (involving the other oxido-O atom) and C–H···π(chelate) interactions as well as π···π stacking between pyridyl and fluorophenyl rings. Of particular interest is presence of the C–H···π interactions as the π-system is defined by the $VSCN_2$ chelate ring, Fig. S27 (b). Such C–H···π (chelate) synthons are gaining increasing recognition in the crystallographic literature, and in fact were probably first recognized in rings containing sulfur.[R1-R4] Globally, the structure can be described in terms of columns of dimeric aggregates parallel to the *c*-axis connected by amine-N–H···O(oxido) and C–H···O(oxido) interactions; different views of the unit cell contents are shown in Figs. S27 (c) and S28.

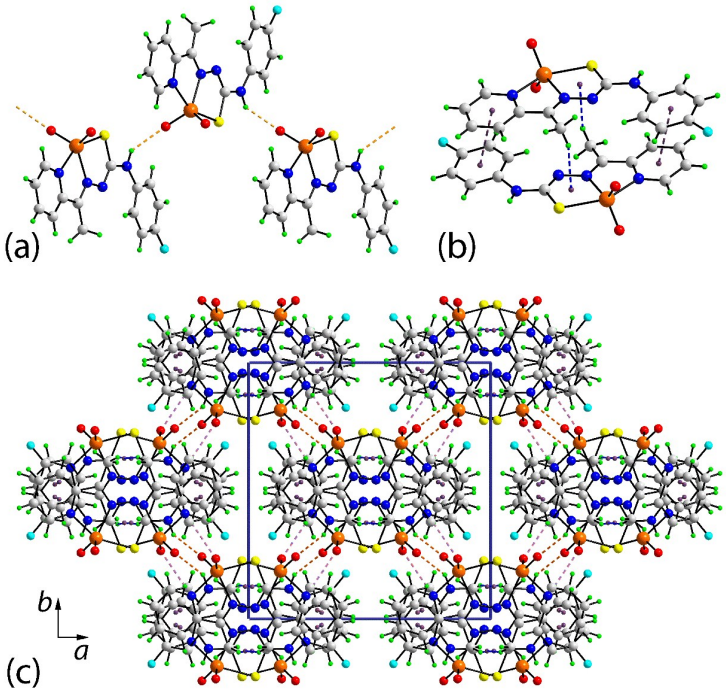

Fig. S27. Molecular packing in **2**: (a) view of the supramolecular zigzag chain mediated by N–H…O hydrogen bonding and orientated along the *a*-axis, (b) dimeric aggregate sustained by methyl-C–H···π (chelate) and π(pyridyl)···π(fluorophenyl)interactions, and (c) view in projection down the *c*-axis of the unit cell contents. The N–H···O, C–H···O, C–H···π, and π···π interactions are shown as orange, pink, blue, and purple dashed lines, respectively.

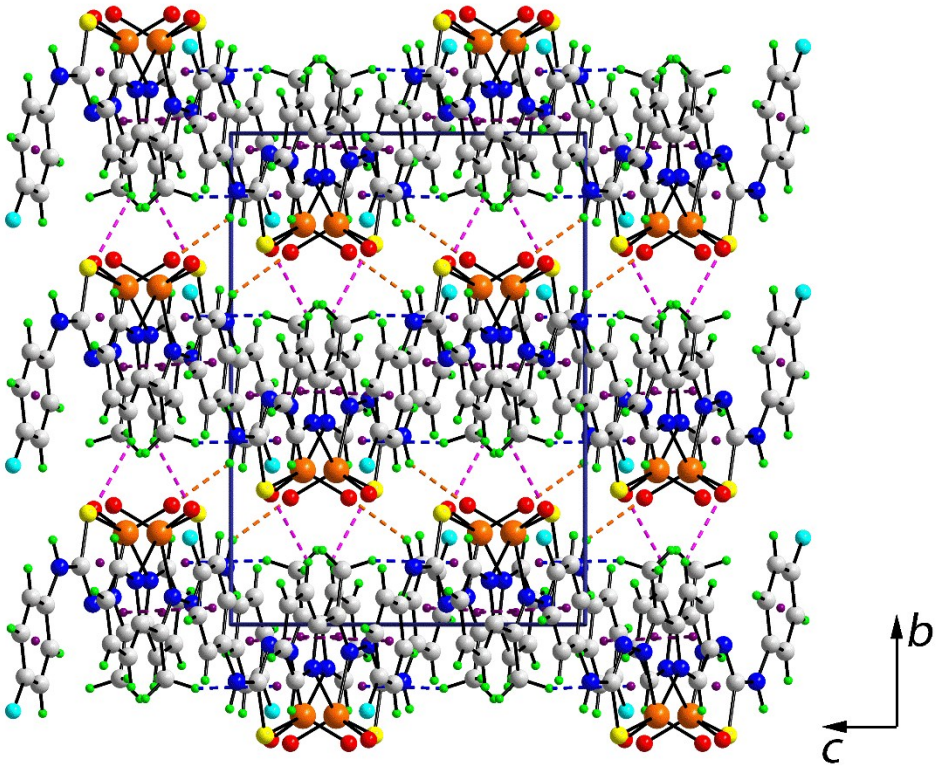

Fig. S28. Molecular packing diagram for **2**: view of the unit cell contents in projection down the *a*-axis. Details of the supramolecular association: N-H···O (orange dashed lines) N1–H1···O1^{i} = 2.22(4) Å, N1...O1^{i} = 2.959(4) Å and, angle at H1 = 142(3)°. C-H···O (pink dashed lines) C11–H11a···O2^{ii} = 2.47 Å, C11···O2^{ii} = 3.173(5) Å and angle at H11a = 133°. C-H···π (blue dashed lines) C9–H9b···π(VSCN$_2$)^{iii} = 2.77 Å, C9···π(VSCN$_2$)^{iii} = 3.647(5) Å and angle at H9b = 152°. π···π (purple dashed lines) Cg(C1-C6)···Cg(N4,C10-C14)^{iii} = 3.514(7) Å and angle of inclination = 4.0(5)°. Symmetry operations - *i*: -½+*x*, ½-*y*, -½+*z*; *ii*: 1½-*x*, ½+*y*, 1½-*z*; *iii*: 1-*x*, 1-*y*, 1-*z*.

The molecular packing of **3** features myriad of points of contact between the constituent molecules; geometric details are given in the caption to Fig. S26. The most prominent interactions are amine-N–H···N(thiadiazolyl) hydrogen bonds between the two molecules comprising the crystallographic asymmetric unit, leading to eight-membered {···HNCN}$_2$ supramolecular synthons; these are flanked by fluorophenyl-C–H···N(thiadiazolyl) interactions. The resultant dimeric aggregates are connected into a

linear supramolecular ribbon along the *c*-axis by pyridyl-C–H···F interactions as shown in Fig. S29 (a). Centrosymmetrically related ribbons are connected into double ribbons by π···π stacking interactions between S1-thiadiazolyl rings, and between N4-pyridyl and S2-thiadiazolyl rings, as well as F···π (fluorophenyl) interactions, Fig. S29 (b). The double ribbons are connected into a three dimensional architecture *via* pyridyl-C–N···π (fluorophenyl) interactions, Fig. S29 (b).

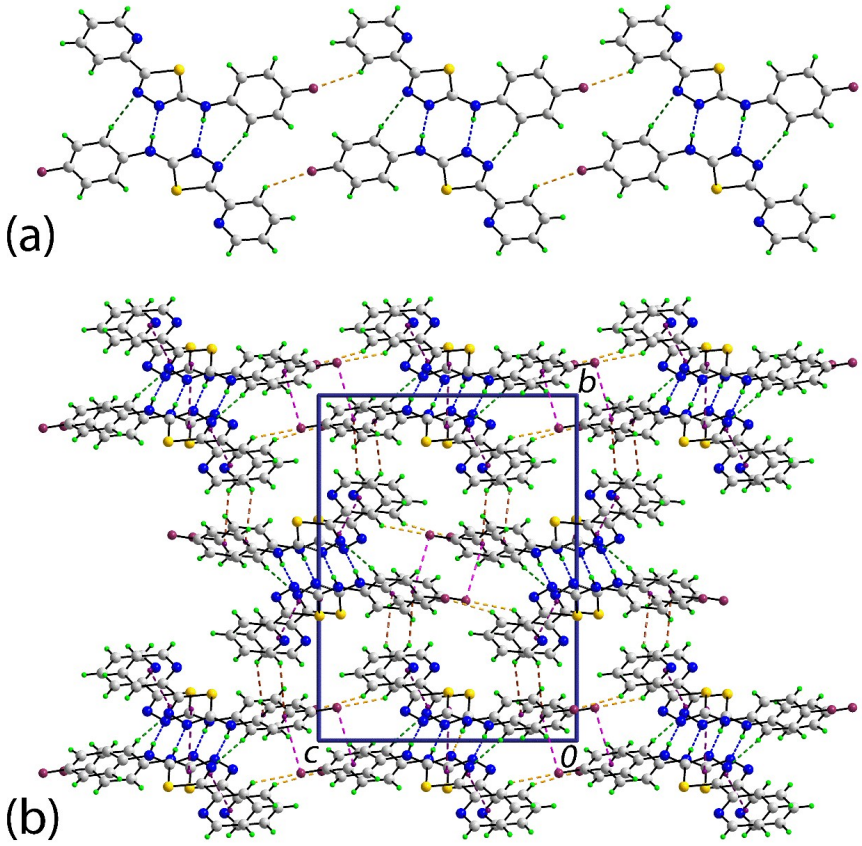

Fig. S29. Molecular packing in **3**: (a) view of the supramolecular ribbon along the *c*-axis, and (b) view in projection down the *a*-axis of the unit cell contents. The N-H···N, C–H···N, C-H···F, π···π, C-F···π and C-H···π interactions are shown as blue, green, orange, pink, purple, and brown dashed lines, respectively.